2.22

MECHANISMS FORCING ANTARCTIC SEA ICE VARIABILITY

Marika M Holland[1*], Cecilia M. Bitz[2], Elizabeth C. Hunke[3]

1 National Center for Atmospheric Research, Boulder, CO
2 Polar Science Center, Applied Physics Laboratory, Seattle, WA
3 Los Alamos National Laboratory, Los Alamos, NM

Abstract

The dominant mode of variability in Antarctic sea ice cover exhibits a dipole pattern with anomalies of one sign in the Pacific and of the opposite sign in the Atlantic. This mode of variability has been documented in observations. Here we examine 550 years of a control simulation of the Community Climate System Model 2 to determine the simulated sea ice area variability and the mechanisms driving this variability. The dominant modes of simulated variability compare well to the observations both in their spatial distribution and magnitude.

The mechanisms driving the simulated sea ice variability are examined. In particular, the interplay of dynamic and thermodynamic processes in forcing the ice variability is discussed. Additionally, how these processes relate to atmosphere and ocean conditions are investigated. The relationships found are consistent with the atmosphere and ocean forcing the sea ice variability, with different processes dominating in the different basins. There are also indications that positive feedbacks associated with the sea ice conditions influence the atmosphere and ocean temperatures in the regions. This acts to prolong the life of the anomalies, particularly in the Pacific basin, and can have remote effects in the Atlantic due to the transport of anomalous ocean conditions by the mean ocean circulation.

1. INTRODUCTION

Sea ice has the potential to affect global climate through its high albedo and influence on the ice/ocean/atmosphere exchange of heat and water. Observations have suggested that variations in the Antarctic sea ice are related to extrapolar climate (e.g. Yuan and Martinson, 2000). In particular, significant correlations exist between Antarctic sea ice and the El Nino-Southern Oscillation (ENSO) (e.g. Simmonds and Jacka, 1995). Additionally, Yuan and Martinson found significant relationships with tropical precipitation, and Indian Ocean sea surface temperatures. However, the observational records of sea ice conditions are relatively short and are occurring during a time of increasing greenhouse gases, which may influence some of these climate relationships.

From the observational studies it is often difficult to determine cause and effect and how feedbacks from the ice cover may influence the atmosphere. However, modeling studies do suggest that variations in Antarctic ice cover can drive atmospheric (Raphael, 2003) and oceanic (Gent et al, 2001) variability.

.* *Corresponding author address*: Marika M Holland, National Center for Atmospheric Research, PO Box 3000, Boulder, CO 80307; email: mholland@ucar.edu

Because of the larger impacts of Antarctic sea ice, it is important to understand what drives variations in the ice cover and in turn how those variations modify the ocean and atmosphere systems. Climate modeling studies can aid in these investigations. While some considerable biases are present in these simulations, they do provide long timeseries of self-consistent data for analysis. If the simulation biases are taken into account, they can provide insight into how the real climate system works.

For this study, antarctic sea ice variability in the Community Climate System Model, version 2 (CCSM2) is examined. In particular, the dominant mode of ice concentration variability and the mechanisms driving this variability are addressed. We focus on the interplay of dynamic and thermodynamic processes in modifying the sea ice conditions. Additionally, the atmosphere and ocean conditions associated with the ice variability are discussed.

2. MODEL DESCRIPTION

Results from a control integration of the Community Climate System Model, version 2 (CCSM2) (Kiehl and Gent, 2002) are examined. This integration is run under present day conditions with no changes in anthropogenic forcing. 550 years of model integration are analyzed

(Years 350-900). This time period was chosen because many of the initial climate drifts in the ice and ocean are considerably reduced by year 350.

CCSM2 is a state-of-the-art coupled general circulation model (GCM) that includes atmosphere, ocean, land, and sea ice components. The model has changed significantly from its initial version (Boville and Gent, 1998), with the sea ice and land components being completely modified. This has led to considerable improvements in the polar regions.

The community land model (Bonan et al., 2002) is the land surface component used within the CCSM2. The model includes a sub-grid mosaic of land cover types and plant functional types derived from satellite observations, a 10-layer soil model that explicitly treats liquid water and ice, a multi-layer snow pack model and a river routing scheme.

The ocean component of the CCSM2 utilizes the parallel ocean program (POP) with a number of improvements (Smith and Gent, 2002). In particular, the model uses anisotropic horizontal viscosity, an eddy mixing parameterization (Gent and McWilliams, 1990), and the K-profile parameterization for vertical mixing (Large et al., 1994). The equations of motion are formulated and discretized to allow the use of any locally orthogonal horizontal grid. As such, both the ocean and sea ice systems use a grid which smoothly displaces the model north pole into Greenland, avoiding problems related to converging meridians in the Arctic. The horizontal resolution averages less than one degree.

The community sea ice model incorporated into CCSM2 is a new dynamic-thermodynamic scheme that includes a subgridscale ice thickness distribution (Bitz et al., 2001; Lipscomb, 2001). The model uses the energy conserving thermodynamics of Bitz and Lipscomb (1999) which has multiple vertical layers and accounts for the thermodynamic influences of brine pockets within the ice cover. The ice dynamics utilizes the elastic-viscous-plastic rheology of Hunke and Dukowicz (1997) with a number of updates. Five ice thickness categories are included within each gridcell and subgridscale ridging and rafting of sea ice is parameterized following Rothrock (1975) and Thorndike et al. (1975). A reasonable Arctic sea ice simulation is present in the control integration. The ice area compares very well to observations. However, the ice is relatively thin which is consistent with biases in the atmospheric radiative forcing at high latitudes (B. Briegleb et al., manuscript in preparation, 2003).

The atmospheric component of the CCSM2 is the community atmosphere model (CAM2). It builds on the NCAR atmospheric general circulation model, CCM3 (Kiehl et al., 1996) with a number of improvements and updates. The model has enhanced resolution in the vertical, going from 18 to 26 levels. Other physics improvements include incorporation of a prognostic formulation for cloud water, a generalized geometrical cloud overlap scheme, more accurate treatment of longwave absorption/emission by water vapor, and enhancements to the parameterization of deep cumulus convection. The model is generally run at T42 (~2.875^{o}) resolution.

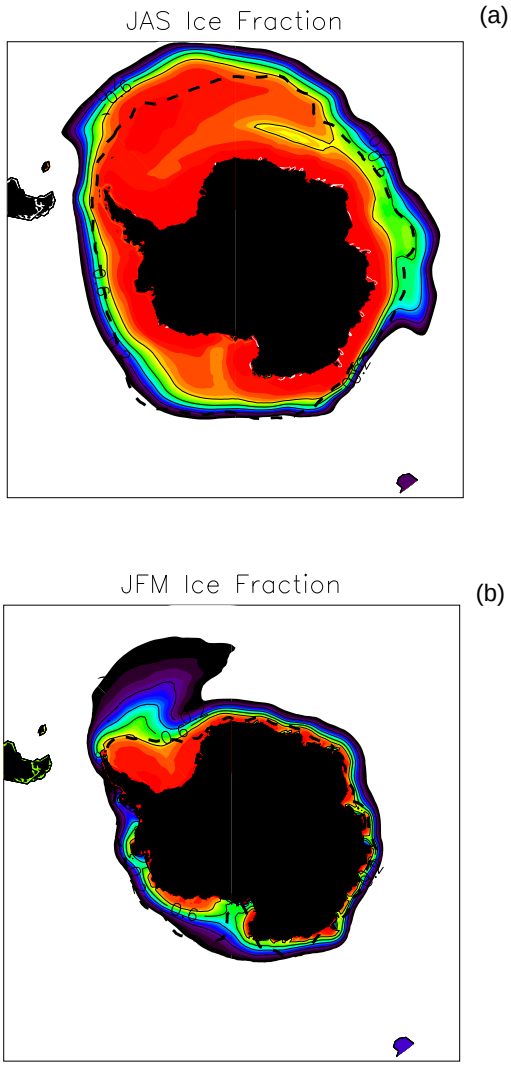

Figure 1. The mean (a) summer and (b) winter ice concentration simulated by the model. The contour interval is 20%. Also shown is the SSM/I 10% ice concentration contour as a dashed line.

3 SIMULATED ICE CONDITIONS

3.1 *Mean conditions*

The CCSM2 control integration obtains a reasonable simulation of southern hemisphere ice area compared to observations. Figure 1 shows the winter and summer ice

area averaged over the last 100 years of the integration with a comparison to the climatological passive microwave satellite observations. The total simulated sea ice coverage is somewhat larger than the observed. Additionally, there are compensating biases in the CCSM2 sea ice spatial distribution, with excessive ice cover in the Atlantic sector and reduced ice cover in the Pacific sector compared to observations. The southern hemisphere ice thickness is also relatively thick, particularly in the Weddell Sea. This is in contrast to biases in the northern hemisphere where the ice is typically thinner than observed estimates (Briegleb et al., 2002). The relatively thick southern hemisphere ice cover results in part from biases in the atmospheric and ocean conditions in this region. The extensive Atlantic ice cover is partly related to the ice thickness bias due to the excessive ice volume that is transported equatorward in the Weddell Sea. The ice velocity appears reasonable in this region, indicating that the high northward ice volume transport is a consequence of the ice thickness.

The relatively low ice area in the Ross Sea region near 135W is related in part to the ocean circulation and the path of the Antarctic Circumpolar current (ACC). The simulated ACC does not accurately capture the equatorward deflection associated with submarine ridge systems in this region (Frank Bryan, personal communication). This possibly results from inadequate resolution of the ocean bathymetry. Because of these biases in the ACC path, the oceanic polar front is located too far poleward. The path of the ACC and resulting sea surface temperature and sea ice conditions in this region slowly evolve over the course of the 1000 year control integration analyzed here, with the ice cover becoming gradually more extensive as the ACC path migrates northward. This is manifested as a linear trend in the simulated ice cover over the integration. This trend is removed for the analysis shown here.

3.2 *Ice Variability*

Figure 2a shows the first empirical orthogonal function (EOF) of simulated wintertime (JAS) ice area for the southern hemisphere. This leading mode of simulated sea ice variability is characterized by a dipole pattern of enhanced ice cover in the Pacific sector associated with reduced ice cover in the Atlantic sector of the southern ocean. This mode accounts for 19% of the variance. The passive microwave satellite observations from 1979-1999 show a similar dipole pattern (Figure 2b), with anomalies of similar magnitude. The observed mode accounts for 30% of the variance. The observed "Antarctic Dipole" pattern has been discussed by Yuan and Martinson (2001; 2000) and has been related to ENSO variability. Because of the compensating anomalies in the Pacific and Atlantic sectors that are associated with this leading mode of variability, it has little correlation to the timeseries of total southern hemisphere ice area.

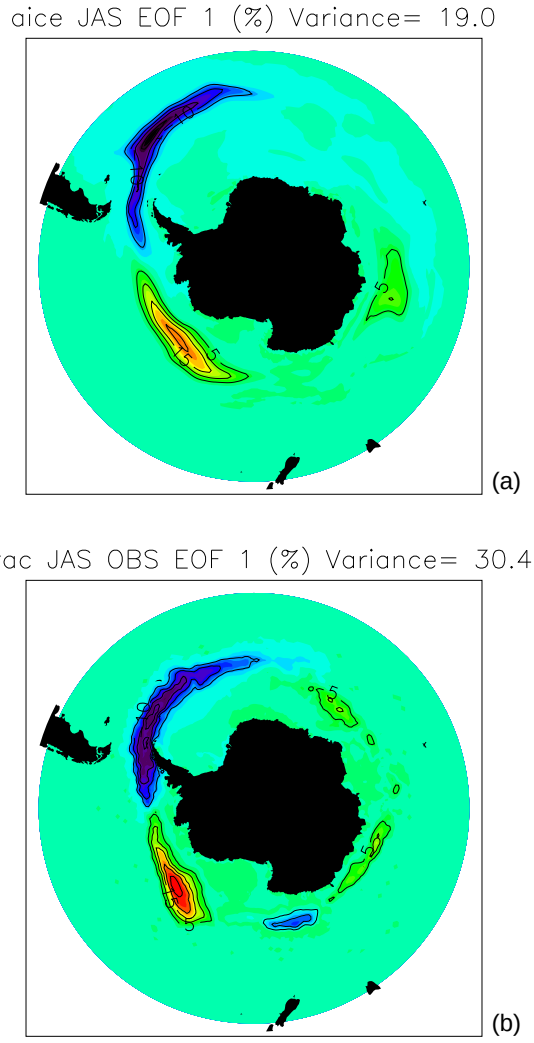

Figure 2. The leading mode of winter ice variability from a) the model and b) satellite observations.

4. MECHANISMS FORCING ICE VARIATIONS

Based on the above analysis, the dominant mode of southern hemisphere winter ice variability present in the CCSM2 is very similar to the limited observational record. This gives some confidence that the simulated mechanisms driving this variability are also realistic. Those mechanisms are discussed here. In particular, we focus on the Antarctic Dipole pattern and examine the interplay between dynamic and thermodynamic processes in forcing the ice anomalies. A timeseries of the Antarctic Dipole is defined as the principal component of the leading mode of wintertime sea ice variability. The atmospheric and oceanic conditions associated with this ice variability, their role in driving and damping the anomalies, and sea ice related feedbacks that modify these conditions are discussed.

4.1 *Interplay of dynamics and thermodynamics*

In order to diagnose the mechanisms forcing the changes in ice cover associated with the simulated Antarctic Dipole, a budget analysis is performed. The ice area tendency terms due to dynamic and thermodynamic processes that are associated with the Antarctic Dipole are computed for an Atlantic and Pacific region. These regions coincide with areas where the anomalies associated with the first ice area EOF (Figure 2) exceed 10% fractional coverage. The thermodynamic processes include all melt and growth terms including lateral, basal and surface processes. The dynamic processes are everything else that acts to change the ice area including ice transport and ridging and rafting.

Figure 3 shows the Pacific ice area tendency terms regressed on the first ice area EOF as a function of lag for both the winter (JAS) and autumn (AMJ) seasons. In the Pacific, where increased ice cover is associated with the positive phase of the Antarctic Dipole, the anomalous sea ice is largely driven by processes in the preceding autumn. Both dynamic and thermodynamic effects increase the ice cover during this time, with the thermodynamic processes dominating. In the coincident winter, thermodynamic processes continue to increase the ice cover although by a reduced amount compared to the autumn ice growth rates. In contrast, dynamic processes in winter reduce the ice area anomalies. Although there continues to be enhanced transport into the region from the south during the winter, the enhanced transport from the anomaly region northward dominates the budget. Overall, the total winter ice area tendency terms only slightly increase the anomalies.

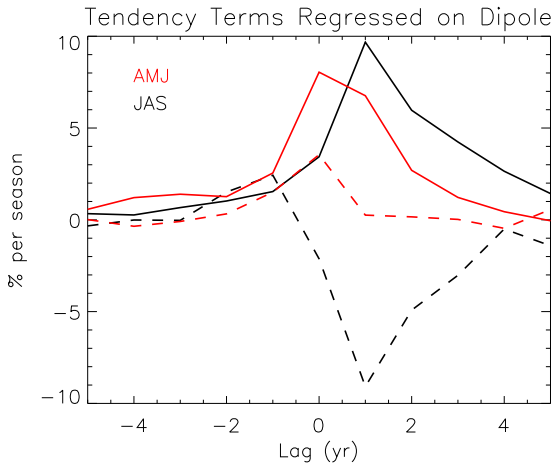

Figure 3. The ice area tendency terms regressed on the Antarctic Dipole. Shown are the tendency due to thermodyanic (solid) and dynamic (dashed) processes for a Pacific region where the ice anomalies associated with the Antarctic dipole exceed 10% fractional coverage.

Curiously, whereas the regression of the ice area tendency terms in autumn are a maximum at zero lag, the winter values show a maximum when they lag the ice EOF by a year. This indicates that changes in ice area due to winter ice growth remain anomalously high in the Pacific following the dipole timeseries. This results from a reduction in winter basal melting in the region at one year lag. As shown below, this is related to the positive ice-albedo feedback which results in colder ocean temperatures. Although, in the Pacific, the increase in ice area due to thermodynamic processes is larger following the Dipole timeseries, the total tendency terms are reduced because of the excessive loss of ice from this region due to dynamics. This increased dynamical ice loss results from a reduction in the northward transport into the region compared to conditions at zero lag, while the eastward ice export out of the region remains high. Thus, dynamic processes, which initially enhance the ice anomalies, eventually counteract the thermodynamic processes, thereby damping the ice anomalies.

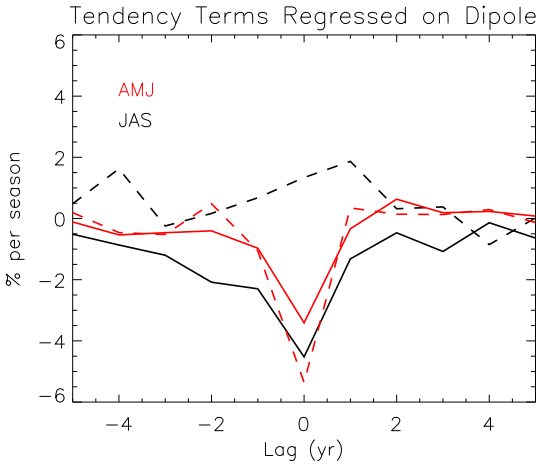

Figure 4. The ice area tendency terms regressed on the Antarctic Dipole timeseries. Shown are the tendency due to thermodynamic (solid) and dynamic (dashed) processes for an Atlantic region.

The Atlantic anomalies which show reduced ice cover associated with the Antarctic Dipole are also driven by changes in the ice area in the preceding autumn (Figure 4). The decreased ice cover is both dynamically and thermodynamically driven. However, in contrast to the Pacific, the dynamical processes dominate. Reduced ice area changes due to low ice growth continue into the winter, whereas dynamical processes act to slightly decrease the anomalies (or increase the ice cover) during the winter. While there is still reduced transport of sea ice into the anomaly region from the south during the winter season, there is also less eastward transport out

of the region and this dominates the total budget. In terms of enhanced thermodynamic growth rates, the Atlantic appears to have less "memory" than the Pacific and the sea ice anomalies are shorter-lived. This is consistent with different ocean conditions between the two basins as shown below.

4.2 *Associated atmosphere conditions*

Both dynamic and thermodynamic processes are important for driving the ice anomalies associated with the Antarctic Dipole. Presumably these processes are related to the atmosphere and ocean state. Additionally, feedbacks associated with the sea ice anomalies can modify the atmosphere and ocean conditions. Those conditions are examined here to determine their relationship to the sea ice variability associated with the Antarctic Dipole
.

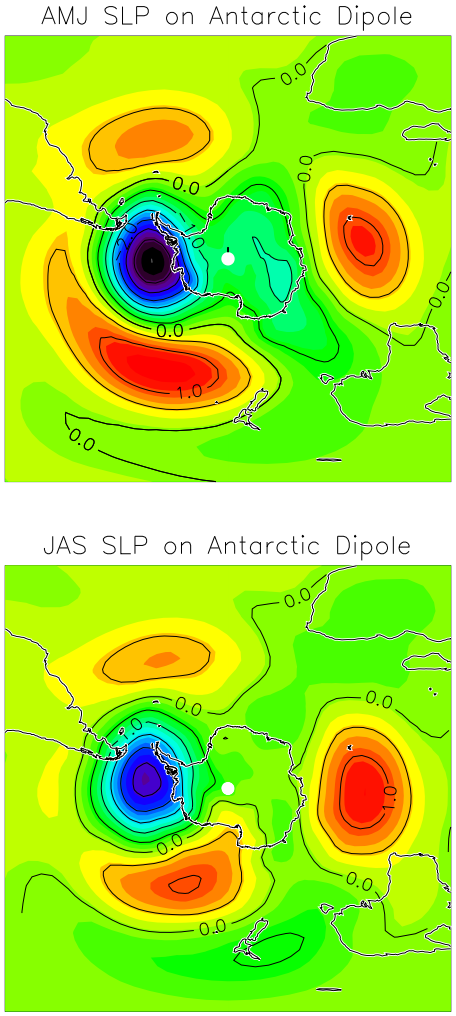

Figure 5. The (a) AMJ and (b) JAS SLP regressed on the normalized Antarctic Dipole timeseries. The contour interval is 0.5 mb.

The linear regression of sea level pressure (SLP) for the preceding autumn and coincident winter on the Antarctic Dipole are shown in Figure 5. The units are in mb per standard deviation of the sea ice principal component. The analysis shows below-normal SLP centered on the Amundsen/Bellingshausen Sea at approximately 90 W. The simulated anomalies are strongest in the autumn preceding the sea ice dipole timeseries, although they remain throughout the winter with a small eastward shift in their location. During autumn, slightly elevated SLP is present northwest of the low SLP anomalies, extending from New Zealand across the Pacific basin at approximately 45 S. These anomalies are centered more directly over the Ross Sea during the winter. The simulated spatial patterns and slow eastward propagation of SLP anomalies associated with the sea ice variations is consistent with atmosphere and sea ice observations as discussed by Kidson and Renwick (2002).

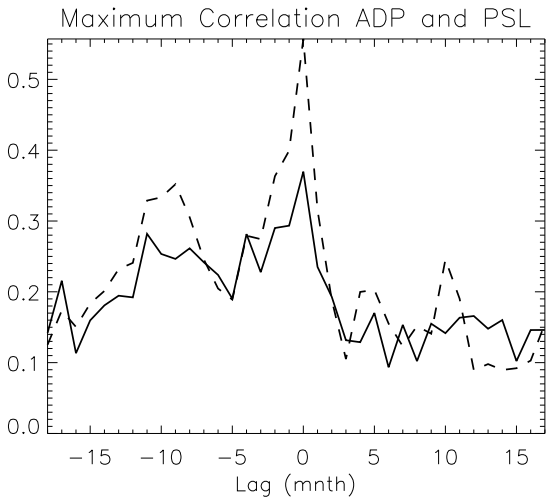

Figure 6. The maximum absolute value of the maximum (solid) and minimum (dashed) correlation between SLP in the southern hemisphere and the Antarctic Dipole as a function of month. Negative lag indicates that the SLP is leading the Antarctic Dipole timeseries.

The geostrophic winds associated with the simulated SLP pattern results in anomalous southerly flow over the Amundsen and eastern Ross Seas and anomalous northerly flow near the Antarctic peninsula. These winds directly drive the ice drift anomalies that were shown above to enhance the Antarctic Dipole anomalies during autumn and indicates that the atmosphere is in part forcing the sea ice variations. As shown by an analysis of the maximum correlations between the monthly SLP and Antarctic Dipole timeseries (Figure 6), there is little indication that the ice anomalies are in turn driving SLP variations and the SLP anomalies associated with the sea ice dipole are minimal by September.

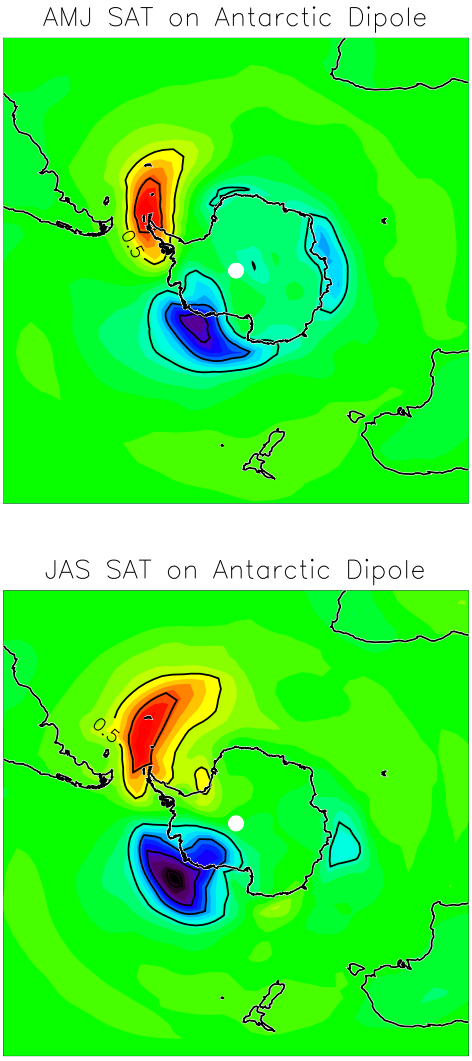

Figure 7. SAT regressed on the Antarctic Dipole for a) AMJ and b) JAS. The contour interval is 0.25 C per standard deviation of the Antarctic Dipole timeseries.

The SLP pattern associated with the Antarctic Dipole also contributes to anomalous atmospheric heat transport, resulting in lower surface air temperatures (SAT) in the Pacific sector and higher temperatures over the Weddell Sea. Figure 7 shows a regression of the SAT on the Antarctic Dipole timeseries. The pattern of colder Pacific and warmer Weddell Sea conditions is clearly evident for both the preceding autumn and coincident winter seasons. This contributes to the thermodynamic forcing of the anomalies. Additionally, as indicated by a correlation analysis, the SAT anomalies associated with the Antarctic Dipole continue into the following year (Figure 8). This is particularly true in the Pacific where negative correlations are present.

Due to the anomalously large ice cover in the Pacific, there is reduced turbulent heat exchange into the atmosphere. This acts to reinforce the SAT anomalies. Directly north of the sea ice anomalies, there is increased turbulent heat flux to the atmosphere due to the cold SAT overlying relatively normal ocean conditions. This damps the SAT anomalies north of the ice edge, reducing their spatial extent. Overall, in the seasons following the Antarctic dipole timeseries, the surface turbulent fluxes in the Pacific act to reinforce the SAT anomalies. Additionally, ocean feedbacks discussed below, extend the life of the sea ice anomalies, allowing them to reform in the Pacific in following years. In the Atlantic, the SAT anomalies associated with the Antarctic Dipole are not as large or as long-lived as those in the Pacific. This difference between the Pacific and Atlantic basins is related to coupled interactions and the mean ocean circulation as discussed below.

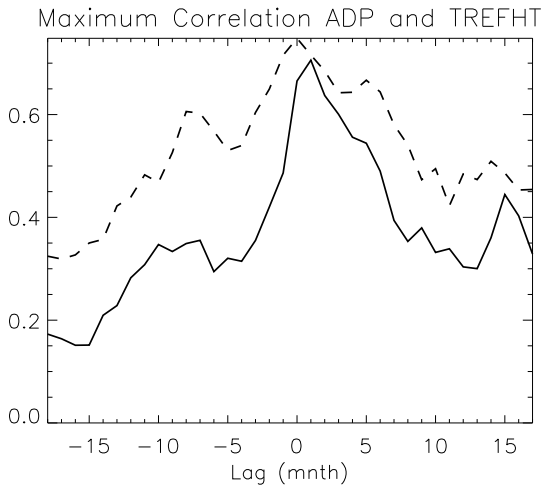

Figure 8. The maximum absolute value of the maximum (solid) and minimum (dashed) correlation between SAT in the southern hemisphere and the Antarctic Dipole as a function of month. Negative lag indicates that the SAT is leading the Antarctic Dipole timeseries.

4.3 *Associated ocean conditions*

Associated with the Antarctic Dipole there are also considerable changes present in ocean conditions. Figure 9 shows the ocean surface currents regressed on the Antarctic Dipole timeseries. Coincident with the ice anomalies, there are changes in ocean circulation particularly in the Pacific which are related to changes in the path of the ACC. This transports more cold water northward away from the Antarctic coast, resulting in reduced ocean heat flux convergence in the Pacific and contributes to the thermodynamic forcing of the sea ice anomalies in this region.

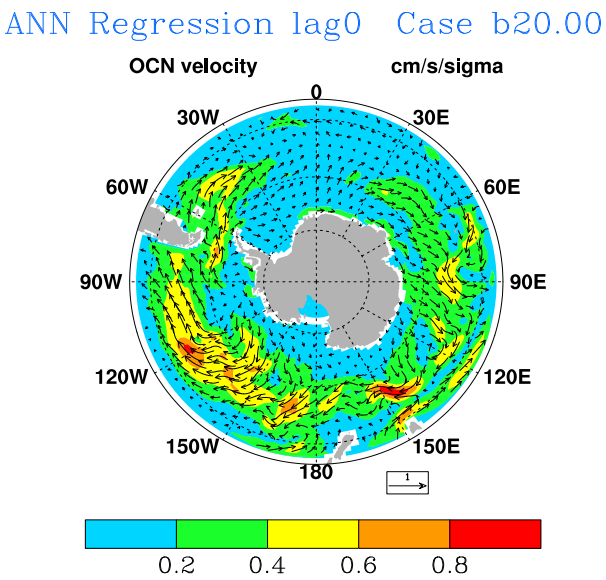

Figure 9. The annual average ocean surface velocity regressed on the Antarctic Dipole timeseries.

Feedbacks associated with the anomalous ice cover in turn modify the surface ocean conditions following the Antarctic Dipole. In particular, the increased ice cover in the Pacific reduces the length of the ice-free season and the solar radiation absorbed by the ocean the following summer (Figure 10). This results in colder SSTs, contributing to the atmospheric SAT feedbacks discussed above, and reducing the ice melt rates in the following year. This allows the ice anomalies to reform in subsequent winters. The anomalies propagate eastward because the SST conditions, and their influence on sea ice and SAT, are transported with the ocean currents.

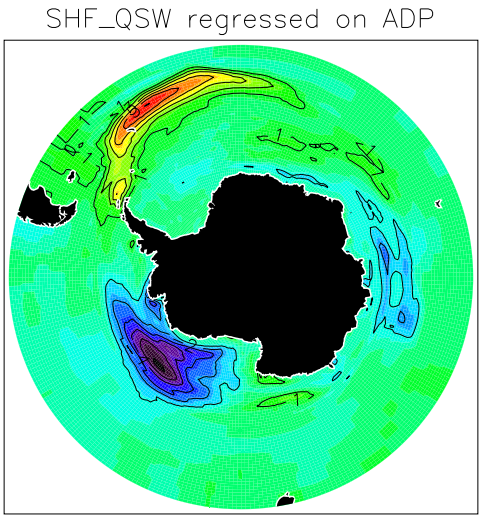

Figure 10. The solar radiation absorbed in the ocean regressed on the normalized Antarctic Dipole timeseries. The contour interval is 1 W m^{-2}.

In the Atlantic, where decreased ice cover is associated with the positive phase of the Antarctic Dipole, more solar radiation is absorbed (Figure 10) and warmer SSTs are present in the region of anomalous ice conditions. However, as mentioned above, this does not appear to reinforce the sea ice or SAT anomalies in the western Atlantic. This is related to the influence of the climatological ocean currents on the anomalous ocean conditions. The mean ocean currents (Figure 11) are relatively strong in the region of the SST anomalies and have a considerable northward component. This transports the warm SSTs to a region where no sea ice formation occurs and hence they no longer have an effect on sea ice conditions. Without this influence, the strength of the turbulent heat flux feedback is reduced and the SAT anomalies are smaller. However, there are indications that the anomalous SST conditions do influence SAT through the turbulent fluxes. In particular, within a year of the anomalous sea ice conditions, an increased turbulent heat flux is present off the southern African coast related to warm SSTs that have been transported to this location from the Weddell Sea. This results in anomalously warm SAT south of Africa. Because the simulated sea ice anomalies in the Atlantic are present relatively far north of their observed values, it is unclear whether a similar mechanism may be driving variability in the real climate system.

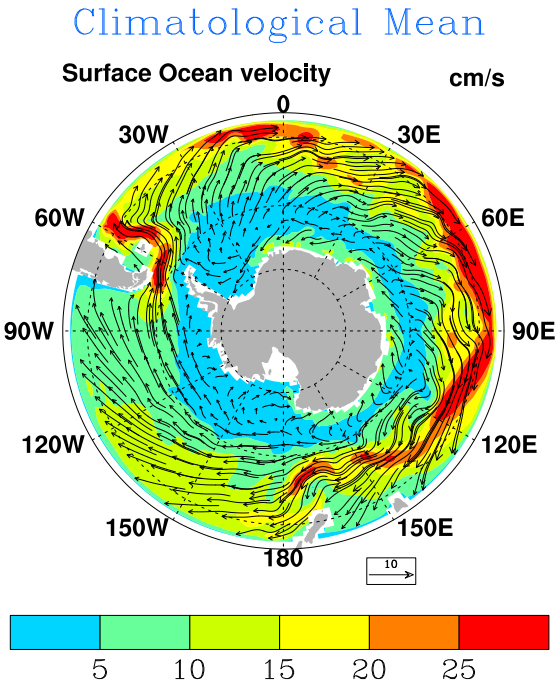

Figure 11. The climatological mean surface ocean velocity in the CCSM2 model.

5. DISCUSSION AND CONCLUSIONS

This study has examined the mechanisms which drive winter sea ice variability in the southern ocean using a control integration of the Community Climate System Model, version 2 (CCSM2). The dominant mode of winter sea ice variability simulated by the model exhibits a dipole pattern with anomalies of opposite polarity in the Pacific and Atlantic basins. This compares well to previous observational studies and an analysis of satellite observations of the ice cover.

In both basins the anomalies are forced by a combination of dynamic and thermodynamic processes in the preceding autumn. The thermodynamic processes dominate in the Pacific, whereas dynamic processes dominate in the Atlantic. The sea ice variability is consistent with SLP variations, indicating that the ice anomalies are partially wind driven. There are also SAT anomalies associated with the sea ice variability that appear to both force and be forced by the ice anomalies.

In the Pacific basin, there are indications that positive feedbacks are important for driving and prolonging the life of the anomalies. In particular, the albedo feedback associated with the changing ice cover, modifies the solar radiation absorbed in the surface ocean. This allows the ice anomalies to reform in subsequent years.

The Atlantic sea ice anomalies have considerably less memory than those in the Pacific. The Atlantic ice anomalies do modify the solar radiation absorbed in the surface ocean the following summer and modify the sea surface temperature conditions. However, the SST anomalies are then transported by the mean ocean currents northward. This removes them to a region where no ice formation occurs, disabling their effect on the Atlantic sea ice conditions.

This study shows that atmosphere and ocean conditions are clearly associated with the antarctic sea ice variability. Initial results suggest that large scale modes of variability such as the El Nino - Southern Oscillation and the Southern Annular Mode influence these variations. Additional work will address the relationships between these large scale modes of variability and the sea ice variations present in the CCSM2.

References:

Bitz, C.M., M.M. Holland, M. Eby, and A.J. Weaver, 2001: Simulating the ice-thickness distribution in a coupled climate model. J. Geophys. Res., 106, 2441-2463.

Bitz, C. M., and W. H. Lipscomb, 1999: An energy-conserving thermodynamic model of sea ice. J. Geophys. Res., 104, 15669-15677.

Bonan, G. B., K. W. Oleson, M. Vertenstein, S. Levis, X. Zeng, Y. Dai, R.E. Dickson, and Z-L Yang, 2002: The land surface climatology of the Community Land Model coupled to the NCAR Community Climate Model. J. Climate, 15, 3123-3149.

Boville, B.A. and P.R. Gent, 1998: The NCAR Climate System Model, version one. J. Climate, 11, 1115-1130.

Gent P. R. and J. C. McWilliams, 1990: Isopycnal mixing in ocean circulation models. J. Phys. Oceanogr., 20, 150-155.

Gent, P.R., W.G. Large, and F.O. Bryan, 2001: What sets the mean transport through Drake Passage?, J. Geophys. Res., 106, 2693-2712.

Hunke E.C. and J. K. Dukowicz, 1997: An Elastic-viscous-plastic model for sea ice dynamics. J. Phys. Oceanogr., 27, 1849-1867.

Kidson, J.W. and J.A. Renwick, 2002: The southern hemisphere evolution of ENSO during 1981-99, J. Climate, 15, 847-863.

Kiehl, J.T., and P.R. Gent, 2002: The Community Climate System Model, Version 2. manuscript in preparation.

Kiehl, J.T., J.J. Hack, G.B. Bonan, B.A. Boville, B.P. Briegleb, D.L. Williamson, P.J. Rasch, 1996: Description of the NCAR Community Climate Model (CCM3). NCAR Technical Note. NCAR/TN-420+STR, 152pp.

Lipscomb, W.H., 2001: Remapping the thickness distribution in sea ice models. J. Geophys. Res., 106, 13,989-14,000.

Large W.G., J. C. McWilliams and S.C. Doney, 1994: Oceanic vertical mixing: A review and a model with a nonlocal boundary layer parameterization. Rev. Geophys., 32, 363-403.

Raphael, M.N., 2003: The impact of observed sea ice concentration on the southern hemisphere extratropical, atmospheric circulation in summer, J. Geophys. Res, submitted.

Rothrock, D.A., 1975: The energetics of the plastic deformation of pack ice by ridging. J. Geophys. Res., 80, 4514-4519.

Simmonds, I, and T.H. Jacka, 1995: Relationships between the interannual variability of Antarctic sea ice and the Southern Oscillation, J. Climate, 8, 637-647.

Smith R. and P. Gent (eds), 2002: Reference manual for the Parallel Ocean Program ocean component of the Community Climate System Model (CCSM2.0). NCAR. Available at http://www.ccsm.ucar.edu/models.

Thorndike, A.S., D.S. Rothrock, G.A. Maykut, and R. Colony, 1975: Thickness distribution of sea ice. J. Geophys. Res., 80, 4501-4513.

Yuan, X and D.G. Martinson, 2000: Antarctic sea ice extent variability and its global connectivity, J. Climate, 13, 1697-1717.

Yuan, X and D.G. Martinson, 2001: The antarctic dipole and its predictability, Geophys. Res. Lett., 28, 3609-3612.